Journal of Chromatography A, 1220 (2012) 35–43

Contents lists available at SciVerse ScienceDirect

Journal of Chromatography A

journal homepage: www.elsevier.com/locate/chroma

Effect of trimethylsilane pre-capping on monomeric C18 stationary phases made from high-purity type-B silica substrates: Efficiency, retention, and stability

Michael D. Bair, John G. Dorsey*

Department of Chemistry and Biochemistry, Florida State University, Tallahassee, FL 32306-4390, USA

ARTICLE INFO

Article history:
Received 9 July 2011
Received in revised form
17 November 2011
Accepted 18 November 2011
Available online 25 November 2011

Keywords:
Stationary phase
C18
Type-B silica
Trimethylsilane pretreatment
Pre-capping
Efficiency

ABSTRACT

Silica-based monomeric C18 stationary phases are the most widely used in reversed-phase liquid chromatography (RPLC), and methods to improve the efficiency and chemical stability of such phases are always being investigated. Previous work showed that stationary phases made by pre-treating the silica surface with small amounts of trimethylsilane (TMS) reagents prior to C18 silanization showed vast improvements in the chromatographic efficiencies of both polar and non-polar analytes. It was concluded that this "pre-capping" step improved efficiency by selectively neutralizing the most reactive highly acidic silanol sites, producing a more energetically homogenous surface prior to exhaustive derivatization that subsequently yielded a more evenly distributed alkyl bonding arrangement. These previous studies were performed on Type-A silica, an older variety of silica gel material that contains higher levels of metal impurities than the Type-B silica used today. The purpose of the work presented here is to investigate the effects of trimethylsilane pre-capping on monomeric C18 stationary phases made from high-purity Type-B silica substrates. The results show little or no efficiency improvements for non-polar compounds, but a more noticeable improvement was observed for some drug compounds and bases under buffered conditions, with the magnitude of the improved efficiencies correlating with metal impurity content and physical parameters of the silica substrate. The results lend supporting evidence that metal impurities are the primary source of highly acidic silanols, but they also suggest a means to improve efficiencies for compounds of interest. Pre-capping also resulted in a decreased retention due to a decrease in carbon loading. In addition, hydrolytic stability of the stationary phases was investigated at high pH and elevated temperature, with results indicating a slight decrease in hydrolytic stability with increased pre-capping.

1. Introduction

Silica-based bonded phases for use in RPLC were first pioneered over 40 years ago by Stewart and Perry [1], and since then many advancements have been made [2–5]. Key to the improvements in chromatographic efficiency and chemical stability exhibited by these phases were advancements in the manufacturing of the porous silica substrate and the synthesis methods used to derivatize the silica surface. Today, properties of silica stationary phases (SP's) including particle size, pore volume, and mean pore diameter can be precisely tailored, and a wide variety of phase modifications are commercially available [6–8].

The chemistry of silica is described extensively in two fundamental texts by Unger [9] and Iler [10]. Amorphous porous silica used for LC SP's is most commonly made via a sol–gel process by which dissolved silicates are polycondensed via the hydrosilation reaction shown in Eq. (1).

$$Si(OR)_{4(aq)} \xrightarrow{H^+,H_2O} SiO_{2(s)} + ROH_{(l)} \quad (1)$$

Type-A and Type-B silicas differ in the starting material used in this process. Type-A silica utilizes silicic acids (R = H), forming water as byproduct. Silicic acids are weak acids capable of leaching and solvating metal cations that then get incorporated into the siloxane polymer network, resulting in contamination of the final silica gel product. Conversely, Type-B silica involves the polycondensation of alkoxy silanes like tetramethoxysilane ($R = -CH_3$) and tetraethoxysilane ($R = -C_2H_5$), forming alcohol as by-product. This process incorporates far fewer metallic impurities into the silica gel product as compared to the Type-A method, and because of this, Type-A materials have fallen out of favor in the last two decades.

The surface features of amorphous silica are depicted in Fig. 1a. Of most importance to the synthesis and chromatographic properties of bonded SP's are silicon-bound hydroxyl groups called silanols, of which there are three varieties – free (i), vicinal (ii), and geminal (iii). Silanols are present on the silica surface at a

* Corresponding author. Tel.: +1 850 644 4496.
E-mail address: dorsey@chem.fsu.edu (J.G. Dorsey).

0021-9673/$ – see front matter © 2011 Elsevier B.V. All rights reserved.
doi:10.1016/j.chroma.2011.11.041

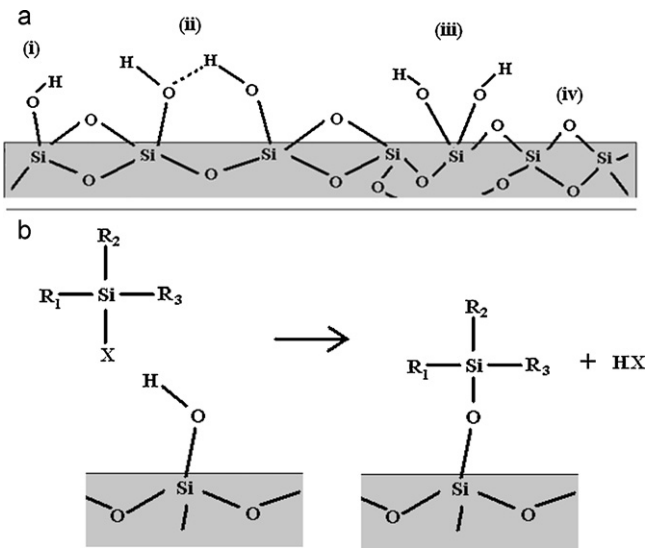

Fig. 1. (a) Silica surface and silanol structure. (b) Monomeric surface derivatization reaction.

concentration of approximately $8 \pm 1\ \mu mol/m^2$, the majority of which are vicinal pairs. Isolated and geminal silanols are generally more reactive than the hydrogen-bonded vicinal variety. Siloxane bridges (iv) present on the silica surface are considered to be inert in terms of reactivity and analyte interaction [9].

Monomeric RPLC stationary phases are made by organically modifying the silica surface via the silanization reaction shown in Fig. 1b, in which a monofunctional silane (a silane reagent with a single leaving group "X," typically a halide) is covalently bonded to the surface at a single silanol site via one siloxane bond (Si–O–Si). Of the three alkyl side chains (–R) on the silane reagent, one is the desired phase modification (R = n-octadecyl for a C18 phase, R = n-octyl for a C8 phase, etc.), while the remaining two are non-functional side chains, usually methyl groups. A weak non-nucleophilic base, like pyridine or 4-DMAP, is employed as a scavenger in the synthesis process to neutralize the acid byproduct and promote a more complete surface coverage. However, despite all attempts to produce RPLC phases with the highest bonded phase coverage possible, a common monomeric C8 or C18 derivatization will only convert roughly 20–50% of all surface silanols to alkyl silanes. In an attempt to further derivatize the unmodified silanols, a smaller and less sterically incumbered silane reagent like trimethylsilane (TMS) is often added after the phase modification in a process called "end-capping." However, end-capping only converts a fraction of the remaining silanols, and residual silanols are always present in the final monomeric bonded phase product.

The roles residual silanols play in the chromatographic properties of silica-based bonded phases have been extensively reviewed [6,11–15]. Chiefly, they give rise to "silanophilic" interactions with certain analytes, particularly amines and other bases. Residual silanols are capable of hydrogen bonding and/or ionic interactions with these analytes, resulting in a mixed-mode retention mechanism that is both thermodynamic and kinetically different than the predominant single-mode solvophobic partitioning of an alkyl RPLC stationary phase. Such heterogeneity in partitioning mechanisms gives rise to broader, more asymmetric peaks, resulting in poorer elution band efficiency.

Less well known but equally important to LC bonded phases is the effect that silanols have on the chemical stability of the silica substrate. High temperature and high pH dissolve the silica support [16], and Unger and Iler both proposed dissolution mechanisms that are kinetically favored at silanol sites [9,10]. Such a mechanism is autocatalytic, as dissolution creates more silanols that then accelerate further dissolution. Therefore, silica materials with a less hydroxylated surface will provide improved stability at elevated temperature and high pH. This has been demonstrated experimentally utilizing thermal dehydroxylation of the silica surface and resulted in slower dissolution under high temperature and basic pH conditions [17].

Silanols are weakly acidic, with most having pK_a's ranging from approximately 3–7, however a small concentration of silanols with pK_a's as low as 2 or 1 have been shown to exist on the silica surface [18,19]. These highly acidic silanols are dubbed "hot spots" since they are more reactive and prone to ionization. While the nature of the amorphous silica surface is quite complex, with various silanol species interacting with each other on a highly curved surface, the source of silanol hot-spots most likely is not inherent to the pure material itself. Instead, the likely culprit is the presence of metal ion impurities, most notably Fe and Al, but also Zn, Cr, Cu and Zr. These metal impurities can be leached from the silica surface by acid-washing the silica in a strong inorganic acid solution (0.1 M to 1.0 M of HCl, H_2SO_4, or HNO_3). However, these metals cannot be removed if they reside deeper within the silica matrix and will inductively draw electron density away from the surface, causing the silanol species in the vicinity of the metal impurity to be more acidic.

Variation in silanol reactivity has effects on the silanization reaction used to synthesize bonded phases. In 1983, Lochmüller et al. used fluorescent pyrene ligands to probe bonded silane distributions on the silica surface and identified clusters of the bonded phase at varying density on the derivatized silica surface [20]. It was suspected that the energetic heterogeneity of the surface silanols led to a less evenly distributed ligand arrangement, with the bonded phase clustering in higher density around the highly reactive silanol hot-spots.

In the years shortly following, D.B. Marshall and Lochmüller showed that pretreatment of the bare silica with small amounts of trimethylsilane (TMS) reagents prior to C18 derivatization resulted in stationary phases with improved retention and efficiency [21,22]. Trimethylsilanes were chosen due to their small size, thus minimizing steric hindrance of neighboring silanol sites for further C18 attachment. They were able to conclude that TMS was selectively neutralizing the most reactive silanols first, leaving a more energetically homogenous surface that then caused the subsequent C18 ligands to bind in a more random, evenly distributed fashion. As a result, the C18 stationary phase products improved analyte efficiency by a factor of 2–3 upon "pre-capping" with TMS at approximately 5–7.5% [21].

To date, all investigations into the effects of pre-capping on silica-based monomeric bonded phases have been performed on Type-A silica. It has since been argued that the presence of silanol hot-spots and their effects on bonded ligand density heterogeneity is a direct result of the presence of metal contaminates, and because Type-B materials lack these sites to any considerable degree, any pre-capping effects should be minimal. However, no experimental data regarding pre-capping Type-B silica phases has yet been reported, but it warrants investigating because it potentially offers a simple and economical way to improve the chromatographic properties of current silica-based bonded phases.

The purpose of the work presented here is to measure the effects of TMS pre-capping on the chromatographic properties of C18 monomeric phases made from Type-B silica. In this study, three different Type-B silica supports were pre-treated with varying amounts of trimethylchlorosilane (TMCS) prior to exhaustive C18 modification, and the efficiency and retention properties of the bonded stationary phase products were measured. Also, the chemical stability of the phases was tested by forced degradation at elevated pH and temperature.

2. Experimental

2.1. Materials and reagents

The three Type-B chromatographic-grade porous silica substrates used in this study were obtained from two different manufacturers: Symmetry® 5 μm from Waters Corp. (Milford, MA, USA), and AstroSil® 14 μm and 7.3 μm from Stellar Phases Inc. (Yardley, PA, USA). Specifications for these silica products as supplied by the manufacturers' Certificates of Analysis (CofA's) are listed in Table 1. Trimethylchlorosilane (TMCS) and n-octadecyldimethylchlorosilane (ODCS) silanizing reagents were purchased from Gelest Inc. (Tullytown, PA, USA). Anhydrous pyridine and dichloromethane (DCM) reagents were purchased from Sigma–Aldrich Corp. (St. Louis, MO, USA). HPLC grade acetonitrile (ACN) and methanol (MeOH) were obtained from Mallinckrodt Baker (Phillipsburg, NJ, USA). Deionized (DI) water was purified to a resistance of approximately 18 MΩ/cm using a NANOPure II water purification system from Barnstead (Debuque, IA, USA). Analyte solutes were obtained from various commercial sources.

2.2. Stationary phase synthesis and column packing

The silica materials were acid-washed in 0.1 M HNO_3 at 80 °C for 4 h, thoroughly rinsed with DI water until the filtrate was pH neutral, dried under vacuum at 150 °C for at least 96 h, then stored in a desiccator. Great care was taken to avoid water and to ensure quantitative TMCS pre-capping in synthesizing the stationary phases. All synthesis glassware was presilanized with a 5% solution of TMCS in anhydrous DCM, dried at 150 °C under vacuum, then assembled hot onto a Schlenk gas/vacuum reaction manifold under dry N_2. In order to minimize error in batch-to-batch synthesis reproducibility, all phases were made in a single-pot fashion, with reagents added sequentially onto the substrate without intermediate isolation. Approximately 5 g of silica was accurately weighed, loaded into a 250 mL flask equipped with a side-arm and septum, then dried on the manifold at 150 °C under vacuum for at least 40 h. Approximately 50 mL of DCM was cannelated onto the dry silica and begun stirring and gently refluxing at 34 °C. TMCS pre-capping was conducted between 0% and 10% silanol equivalents calculated using the exact mass of dry silica (g), the manufacturer-specified BET surface area (m^2/g), and assuming 8.0 μmol/m^2 surface silanol concentration, resulting in 100% silanol equivalents of 2.7 mmol/g for the Symmetry 5 μm material, and 2.6 mmol/g and 2.8 mmol/g for the AstroSil 14 μm and 7.3 μm materials, respectively.

For the TMS pre-capping step, a 1:50 (v/v) TMCS:DCM (anhyd.) solution was freshly prepared and the appropriate amount was introduced dropwise to the stirring/refluxing reaction slurry via gas-tight syringe, followed immediately by an excess amount (>120% silanol equivalents) of anhydrous pyridine. This was allowed to react for 6 h prior to exhaustive C18 silanization with ODCS for 18 h. Most stationary phases were subsequently endcapped with an excess amount of TMCS for 24 h. A 2.5% "dilution phase" (2.5%dln) was also synthesized in which the C18 and TMS reagents were added simultaneously at a ratio of 97.5:2.5 ODCS:TMCS and reacted for 24 h, then endcapped with excess TMCS, in order to observe the effect of alkyl ligand dilution previously investigated by Marshall et al. [21]. Derivatized silica products were filtered and washed with ample volumes of DCM, methanol, 50:50 water:methanol, and diethyl ether, then dried under vacuum at 125 °C for 6 h. The resulting monomeric C18 stationary phase products were slurry-packed into standard 4.6 mm × 150 mm stainless steel HPLC columns (SciCon or equivalent) at approximately 6000 psi using a Haskel DSTV-122 air-driven pressure amplifier (Burbank, CA, USA) with isopropanol (IPA) used as both the slurry and pushing solvents.

Table 1
Physical parameters and metal impurity content of the bare silica materials used.

	Stellar AstroSil	Stellar AstroSil	Waters Symmetry
Particle diameter (μm)	14	7.3	5
Particle size distribution (dp90/dp10)	1.6	<1.5	1.49
Avg. surface area (m^2/g)	325	350	341
Avg. pore diameter (Å)	106	95	92
Avg. pore volume (mL/g)	0.9	0.8	0.88
%C[a]	0.6	0.4	0.1
Metal impurity content (ppm)			
Na	12	18	<1
Mg	<9	<9	NA
Ca	14	<9	NA
Al	11	15	<1
Fe	<9	<9	1

[a] The % carbon data was measured in this study and not provided on the vendors' CofA.

2.3. Liquid chromatography instrumentation

The van Deemter analysis was performed on an optimized HPLC system designed to minimize extra-column volume and consisted of an LC-10AT VP pump (Shimadzu Manufacturing Inc., Canby, OR, USA), a Waters 486 Tunable Wavelength Detector (Milford, MA, USA), and a Valco manual 6-port injection valve (Houston, TX, USA) with a 10 μL injection loop. van Deemter chromatograms were collected and processed using TotalChrom 6.2.1 software. All other chromatographic experiments were performed on an automated Shimadzu system consisting of an LC-10ADvp pump and DGU-14A mobile phase degasser, SPD-10Avp UV/Vis detector, SIL-10A auto-injector, and a SCL-10Avp system controller. Chromatograms were collected and processed with CLASS-VP v.5.03 software. All injections were 5.0 μL of a 1.0 mg/mL analyte concentration in 1:1 H_2O:ACN diluent under isocratic elution conditions at 1.0 mL/min with uracil as a void marker, unless otherwise noted. The UV detection was at 254 nm with a sampling rate of 5 Hz or greater. Temperature-controlled experiments utilized an Isotemp Refrigerated Circulator Model 9100 (Fisher Scientific, Pittsburg, PA) and a column jacket. Data analysis and graphing were done in Microsoft Excel.

3. Results and discussion

3.1. Stationary phase and packed-column characteristics

Tables 1 and 2 provide information on the silica substrates used in this study and the C18 stationary phases synthesized from them. Note that the Symmetry silica contains considerably less metal impurities than the AstroSil silicas. The batch of AstroSil 14 μm material was available in ample quantity (>500 g), but the AstroSil 7.3 μm and the Symmetry 5 μm batches were both limited (20–30 g). Therefore, more experimentation of the AstroSil 14 substrate was possible, and this material was employed in the early stages of the study to develop column packing procedures and chromatography methods. In total, one batch of the 0% pre-capped (non-precapped) and two batches each of the 2.5%, 5%, 7.5%, and 10% TMS pre-capped phases were made on the AstroSil 14 silica, and multiple columns (1–3) of each batch were successfully packed. Data from these multiple columns were used to gauge the reproducibility of the column manufacturing process.

Table 2 shows the carbon loading of the synthesized C18 phases. Each phase showed a decrease in carbon loading with increased pre-capping, which is a consequence of the diminished number of silanol sites available for the subsequent C18 addition. Note that the

Table 2
List of all C18 stationary phases synthesized, their pre-capping levels, presence or absence of end-capping, and the measured carbon loading as determined by elemental analysis.

	Amount of pre-capping (%TMS)	End-capped (Y/N)	%C (corrected[a])
AstroSil 14 μm	0%	Y	19.2
	0%	N	17.5
	2.5%	Y	17.2 ± 0.0[b]
	2.5%	N	17.0
	5.0%	Y	17.2 ± 0.3[b]
	7.5%	Y	16.2 ± 0.3[b]
	10.0%	Y	16.2 ± 0.5[b]
	2.5%dln	Y	16.9
AstroSil 7.3 μm	0%	Y	16.8
	0%	N	15.8
	2.5%	Y	16.1
	2.5%	N	14.2
Symmetry 5 μm	0%	Y	16.5
	2.5%	Y	14.7
	10.0%	Y	12.6

[a] Corrected %C = measured %C of phase product − measured %C of bare material listed in Table 1. Four repeated measurements of a separate standard C18 phase gave a standard deviation of ±0.3%C for the elemental analysis error.
[b] Average and range of %C for two separate synthesis batches. Each batch measurement was within ±0.5%C of the reported mean, indicating a low batch-to-batch variability of the synthesis process.

2.5% pre-capped phase showed the lowest discrepancy in the %C measured for the two batches synthesized at ±0%C, while the 10% phase showed the greatest discrepancy at ±0.5%C. This suggests that increased pre-capping may introduce greater batch-to-batch variation in carbon loading, but overall the effect is minimal, especially at low levels of TMS pretreatment. The 2.5% "dilution phase" (2.5%dln) was made from AstroSil 14 μm material in a "co-capping" fashion where the TMS and C18 silanes were added concurrently, not sequentially, in order to determine what effects are due to pretreatment and which can be attributed to a simple dilution of the alkyl ligand density.

To ensure adequate column packing quality of the stationary phases, the columns were screened by running an isocratic 40:60 H_2O:ACN method to measure the chromatographic efficiency of various aromatic compounds. All efficiencies were calculated using the Foley–Dorsey equation [23] as shown in Eq. (2):

$$N = \frac{41.7 \times (t_R/w_{0.1})^2}{1.25 + B/A_{0.1}} \quad (2)$$

where t_R is the analyte retention time, and $w_{0.1}$ and $B/A_{0.1}$ are the measured peak width and peak asymmetry at 10% peak height, respectively. Note that this calculation accounts for peak shape (asymmetry), yielding lower calculated plate number with increased tailing (higher B/A).

The efficiencies measured for four non-polar analytes (toluene, ethylbenzene, naphthalene, and anthracene) are shown in Fig. 2. Here again, the results reported for the AstroSil 14 phases are the average of several columns packed with different SP batches at each pre-capping level, while the Symmetry 5 and AstroSil 7.3 show one column from one batch. The efficiency variability for the multiple AstroSil 14 columns packed at each pre-capping level averaged ±11% RSD, with a maximum of ±15% RSD. The column-to-column reproducibility is the principle source of error in this study, thus any difference in efficiency less than ±15% is considered to be within experimental error.

TMS pre-capping offered little or no improvement in the efficiency for non-polar analytes on all phases. The efficiencies on the Symmetry 5 and AstroSil 7.3 phases varied <10%, and peak shape remained between 1.05 and 1.15. For the AstroSil 14 phase, no

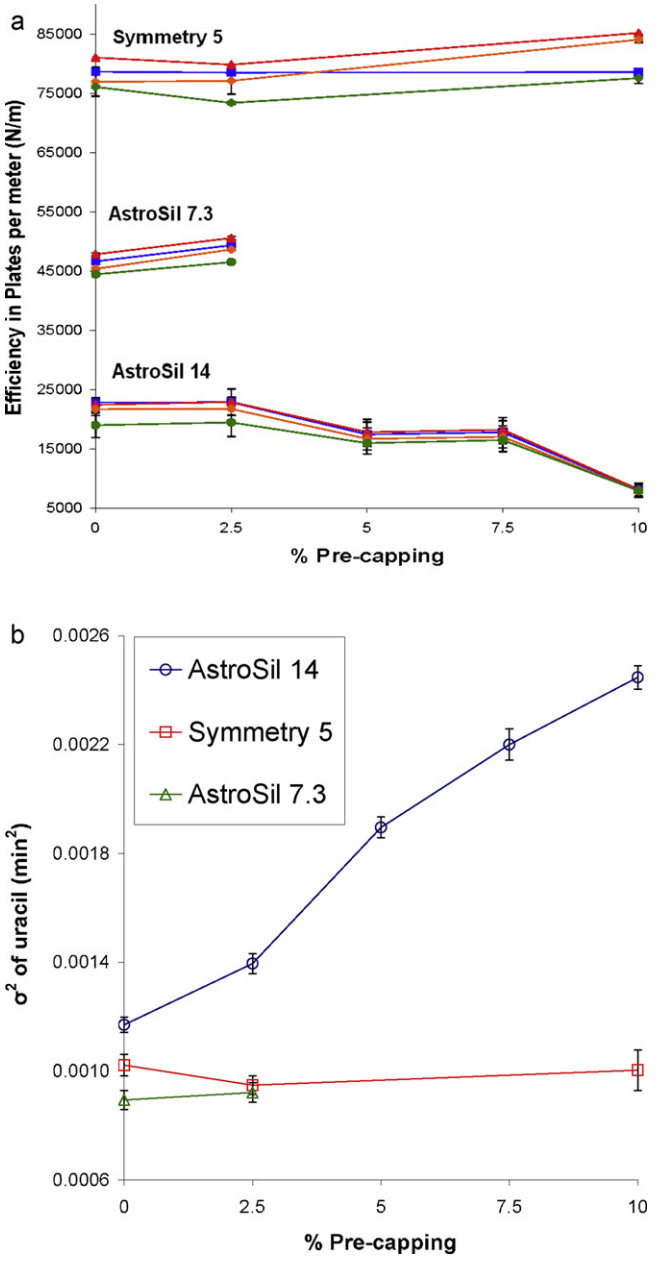

Fig. 2. (a) Measured efficiency of ethylbenzene (■), toluene (▲), naphthalene (◆), and anthracene (●) vs. amount TMS pre-capping for packed columns. Isocratic elution with 40:60 H_2O:ACN at 1.00 mL/min and ambient temperature, 5 μL injection of 1 mg/mL toluene and ethylbenzene, 0.6 mg/mL naphthalene, and 0.04 mg/mL anthracene in 1:1 H_2O:ACN diluent. For the Symmetry 5 and the AstroSil 7.3 phases, error bars show the standard deviation of 5 replicate injections on one column. For the AstroSil 14, error bars show standard deviation of 5 injections from multiple packed columns: 0% = 3 columns total from 1 batch of synthesized phase; 2.5%, 5% and 7.5% = 3 columns total from 2 batches; and 10% = 2 columns total from 2 batches. All stationary phases were endcapped. (b) Second statistical moment variance (σ^2) of uracil void marker for one series of packed columns. Error bars show the standard deviation of 5 replicate injections. (For interpretation of the references to color in this figure legend, the reader is referred to the web version of the article.)

significant change was seen at the 2.5% pre-capped level. At 5% and 7.5%, there is an approximately 20% decrease in efficiency, with a slight increase in peak tailing but still <1.2 on average. However, the 10% pre-capped phase showed a drastic 60% decrease in efficiency and a sharp increase in tailing (>1.5). None of the other packed columns showed this trend. The decrease in efficiency upon increased pre-capping observed for the AstroSil 14 phases is most likely due to poor column packing [24]. It is believed that

the IPA slurry packing method employed is less suitable for larger particle phases with lower carbon loading, and aggregation and/or sedimentation occurs more rapidly during the packing process producing a less homogenous packed-bed.

A statistical moments analysis was performed on all columns to correct for variances in column packing. Adjusted plate numbers (N_{adj}) were calculated by subtracting the variance exhibited by the uracil void-marker (σ^2_{void}) from the analyte peak variance (σ^2_{anal}), giving $N_{adj} = t_R^2/(\sigma^2_{anal} - \sigma^2_{void})$ [21,25]. The variances in the uracil void peak are plotted in Fig. 2b. An increase in σ^2_{void} indicates poorer packing and was only seen for the AstroSil 14 phases. The uracil peak variance changed little for the Symmetry 5 and AstroSil 7.3 phases and their N_{adj} values reflect those shown in Fig. 2a. For the AstroSil 14 phases, the calculated N_{adj} showed a slight maximum at 2.5% pre-capping (6–8% over non-precapped), and the ratio of $\sigma^2_{anal}/\sigma^2_{void}$ was a minimum at this level as well. The N_{adj} values at the 10% level were improved considerably, but overall the trend was the same as that calculated by Eq. (2) and shown in Fig. 2a. While void variance adjustment could not correct for all of the decrease in efficiency observed for the AstroSil 14 phases at 5% pre-capping and higher, this would eventually be considered inconsequential as work began to focus on the 2.5% level as the optimal pre-capping amount to be studied.

3.2. Efficiency

A flow-rate dependent analysis using toluene as the probe analyte was conducted on the endcapped phases to gain more insight into the kinetics governing each phase's efficiency. The results were modeled using the van Deemter equation [26,27],

$$H = A + B/\mu + C\mu \quad (3)$$

where H is the plate height, and μ is the average linear flow rate in calculated from the volumetric flow rate and the uracil void marker elution time. The A, B, and C coefficients are the eddy diffusion, longitudinal diffusion, and mass-transfer terms, respectively. The van Deemter analysis results are presented in Fig. 3 and Table 3.

Several trends can be seen in the van Deemter data. First, the A-term tends to increase while the B-term decreases with increased pre-capping for the AstroSil 14 phases; both are an indication of poorer packing quality. More importantly, the calculated C-term for all three silica substrates was a minimum at the 2.5% pre-capped level, regardless of packing quality. As a result, the 2.5% pre-capped phases generally had the lowest minimum plate height (H_{min}) and the highest optimal linear flow velocity (μ) on all three silica substrates. The van Deemter results confirmed what was observed repeatedly throughout the study, which is that the 2.5% phases generally showed an improvement in efficiency and peak shape over the non-precapped phase for each silica substrate studied.

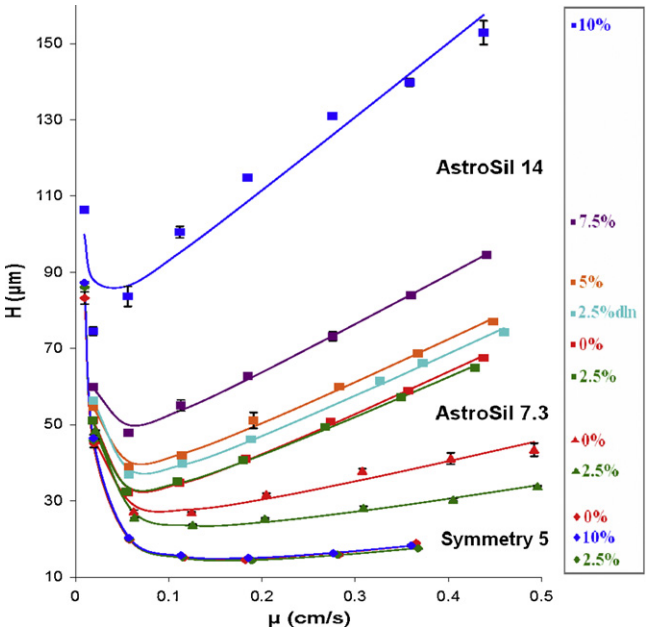

Fig. 3. van Deemter plots for toluene on Symmetry 5 (♦), AstroSil 7.3 (▲), and AstroSil 14 (■) C18 phases at various pre-capping levels. Isocratic elution with 40:60 H_2O:ACN from 0.05 mL/min to 2.50 mL/min at ambient temperature, with uracil as void marker. Error bars show the standard deviation of triplicate injections of 10 µL at 1.0 mg/mL of toluene in 1:1 H_2O:ACN diluent. Smooth line represents the least-squares fit of the van Deemter model from Eq. (3). All stationary phases were endcapped.

This improvement was often negligible (<10%) for the non-polar analytes but more significant for polar analytes.

In practice, improved efficiency and peak shape are most relevant to drug compounds because their polar and often basic structures give rise to broad, tailing peaks [12,15]. Several pharmaceutical analytes were studied under buffered conditions using a 15 mM phosphate buffer at both low pH (2.75) and high pH (6.90). Also, non-endcapped phases at 0% and 2.5% pre-capping were synthesized on the AstroSil materials to compare the relative effects of TMS pre-capping and end-capping on peak shape and efficiency.

A total of ten drug compounds at two buffered pH conditions were screened on the AstroSil 14 and Symmetry 5 phases from 0% to 10% pre-capping, as shown in Fig. 4. For the Symmetry 5 phases, all analytes at both pH conditions showed an insignificant (<15%) improvement in peak efficiency upon TMS pre-capping, with the exception of quinine that showed a 20% improvement upon 10% pre-capping at pH 2.75. Conversely, all analytes on the AstroSil 14 phases showed a maximum efficiency at the 2.5% pre-capping level under both pH conditions, with the exception of Ketoprofen at pH 6.90. In summary, the AstroSil 14 material, which contains a higher level of metal impurities, showed small but

Table 3
Calculated van Deemter parameters for toluene. From Fig. 3.

	Precapping level (%TMS)	A (10^{-3} cm)	B (10^{-5} cm^2/s)	C (10^{-3} s)	μ optimal (10^{-2} cm/s)	H_{min} (µm)	Residual error (µm^2)
AstroSil 14 µm	0%	1.6	6.2	11.6	7.3	32.8	3.3
	2.5%	1.7	5.7	10.9	7.2	33.4	3.5
	5.0%	2.4	5.3	11.7	6.5	39.9	6.5
	7.5%	3.5	4.2	13.3	5.6	49.7	7.1
	10.0%	7.1	2.5	19.6	3.7	84.8	35.6
	2.5%dln	2.1	6.3	11.6	7.4	37.8	3.7
AstroSil 7.3 µm	0%	1.6	5.9	5.8	10.1	27.5	18.9
	2.5%	1.3	7.4	4.0	13.5	23.5	3.6
Symmetry 5 µm	0%	0.5	7.6	3.1	15.6	14.7	1.1
	2.5%	0.5	7.8	2.8	16.5	14.4	0.1
	10.0%	0.5	7.7	3.0	16.1	14.9	0.1

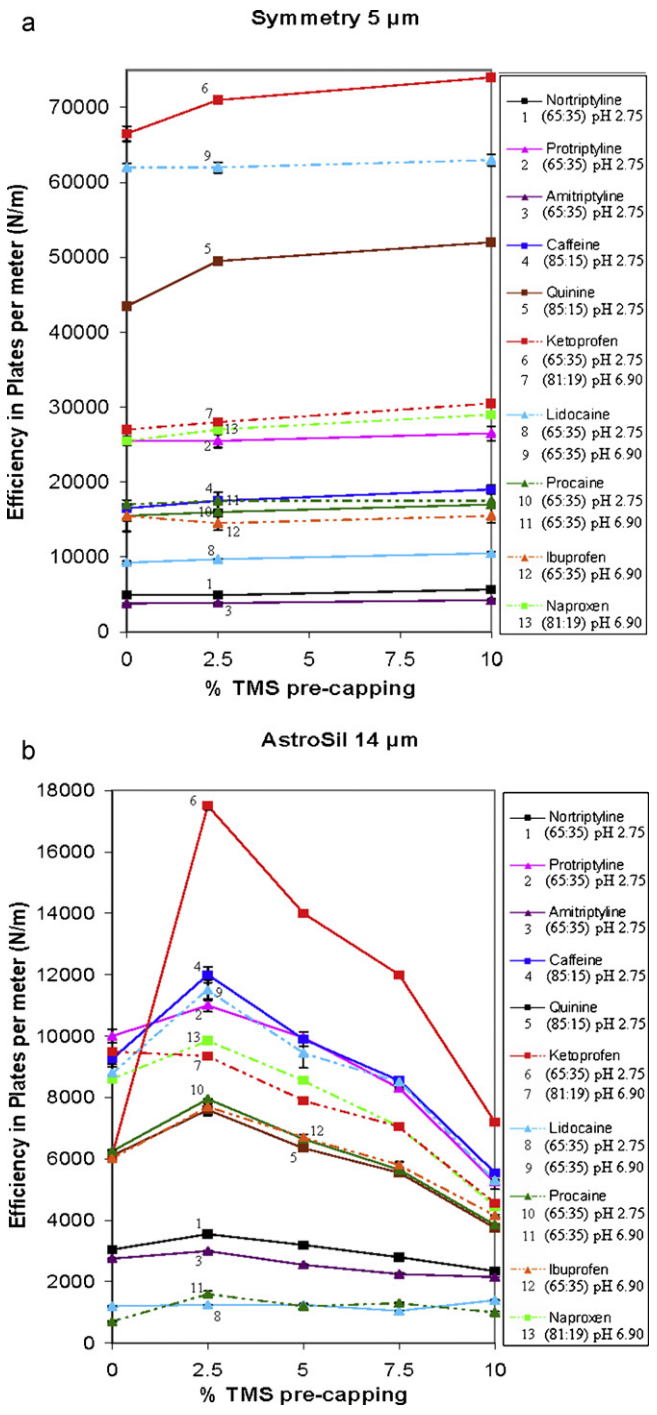

Fig. 4. Efficiency vs. TMS pre-capping for ten drug analytes on (a) Symmetry 5, and (b) AstroSil 14 C18 phases at pH 2.75 (solid line) and pH 6.90 (dashed line). Isocratic elution at 1.00 mL/min at the MP conditions listed (15 mM aqueous phosphate buffer: acetonitrile), 1:1 H_2O:ACN sample diluent, and ambient temperature. Ketoprofen, Lidocaine, and Procaine were analyzed at both pH conditions. Error bars show the standard deviation of triplicate injections. All stationary phases were endcapped.

noticeable improvements in efficiency for some polar compounds, while the highly pure Symmetry material showed no significant improvement for almost all analytes studied.

Fig. 5 shows how the efficiency and peak shape vary with both pre-capping and end-capping for the two AstroSil materials. For the 14 µm phases (Fig. 5a), pre-capping at 2.5% showed an equivalent or improved peak shape (B/A closer to 1) for both the end-capped and non-endcapped phases, and improvements were seen in the efficiencies as well. In general, end-capping outperformed pre-capping alone, but the combination of 2.5% pre-capping and endcapping improved efficiency over end-capping alone by ≥25% for all analytes shown in Fig. 5. However, some of these same effects were seen on the 2.5% dilution phase, indicating that gains in efficiency and peak shape upon pre-capping for many of these analytes can be attributed in part to a more dispersed C18 alkyl arrangement and not necessarily a result of the TMS-pretreatment's neutralization of reactive silanols prior to C18 derivatization.

Many of the trends seen for the AstroSil 14 µm phases were less apparent on the 7.3 µm phases shown in Fig. 5b. Improvements in peak shape were less noticeable on the 7.3 phases, and the combination of pre-capping and endcapping only showed an insignificant (<10%) improvement in efficiency vs. endcapping alone. A potential reason for this can be seen in Tables 1 and 2. While both AstroSil phases are *chemically* similar in terms of their metal impurity profiles, the 7.3 µm material is more similar to the Symmetry 5 µm material *physically* in terms of particle diameter, surface area, and most importantly average pore diameter. Narrow pores restrict silane reagents from accessing the silica surface, resulting in a decrease in overall carbon loading for silica materials with a smaller average pore diameter. This effect is most significant with pore diameters less than 140 Å and with longer alkyl ligand reagents like octadecylsilanes [28,29]. The carbon loading data in Table 2 correlates well with the mean pore diameter data reported in Table 1 for this reason. Thus, if improvements in peak shape and efficiency observed for the drug compounds in Figs. 4 and 5 on the 2.5% pre-capped phases can be attributed in part to a diminished C18 bonding density as evident by the 2.5%dln phase, then those phases with an already low bonding density should exhibit less improvement upon pre-capping, as evident by the AstroSil 7.3 and Symmetry 5 phases. It is now hypothesized that metal impurity content is not the sole indicator of whether TMS pre-capping will improve efficiency on Type-B silica, but physical parameters such as mean pore diameter and how they affect bonded phase density should also be considered.

3.3. Retention

Pre-capping on Type-B silica is shown to decrease carbon loading (Table 2), and this will undoubtedly affect the retention properties for the C18 phase products. Fig. 6 shows the retention factors (k') of ethylbenzene and toluene as a function of pre-capping. Retention of these analytes was maintained upon 2.5% pre-capping, however a sharp decrease in k' was observed at higher levels. Other non-polar compounds analyzed including benzene, naphthalene, and anthracene showed similar retention loss. This result is in stark contrast to the trend observed on Type-A silica, which typically showed an increase in carbon loading and retention up to ~5% pre-capping [21].

To obtain retention thermodynamic data, a van't Hoff analysis was conducted. Plots of $\ln k'$ vs. inverse absolute temperature $1/T$ ($1/K$) yield linear plots as per Eq. (4), where the standard enthalpy (ΔH°) of solute partitioning from mobile phase (MP) to stationary phase (SP) can be calculated from the observed slope.

$$\ln k' = \frac{-\Delta H^\circ}{RT} + \frac{\Delta S^\circ}{R} + \ln \varphi \quad (4)$$

The y-intercept term comprises both the standard entropic contribution of retention (ΔS°) and the volumetric phase ratio ($\varphi = V_{SP}/V_{MP}$). These two quantities cannot be measured directly, but a method to derive entropic information was proposed by Coym and Chester [30]. Assuming two analytes that differ only by a methylene group ($-CH_2$) experience the same phase ratio, subtracting-out the y-intercept term of two homologous compounds (in this case, ethylbenzene and toluene) removes the phase

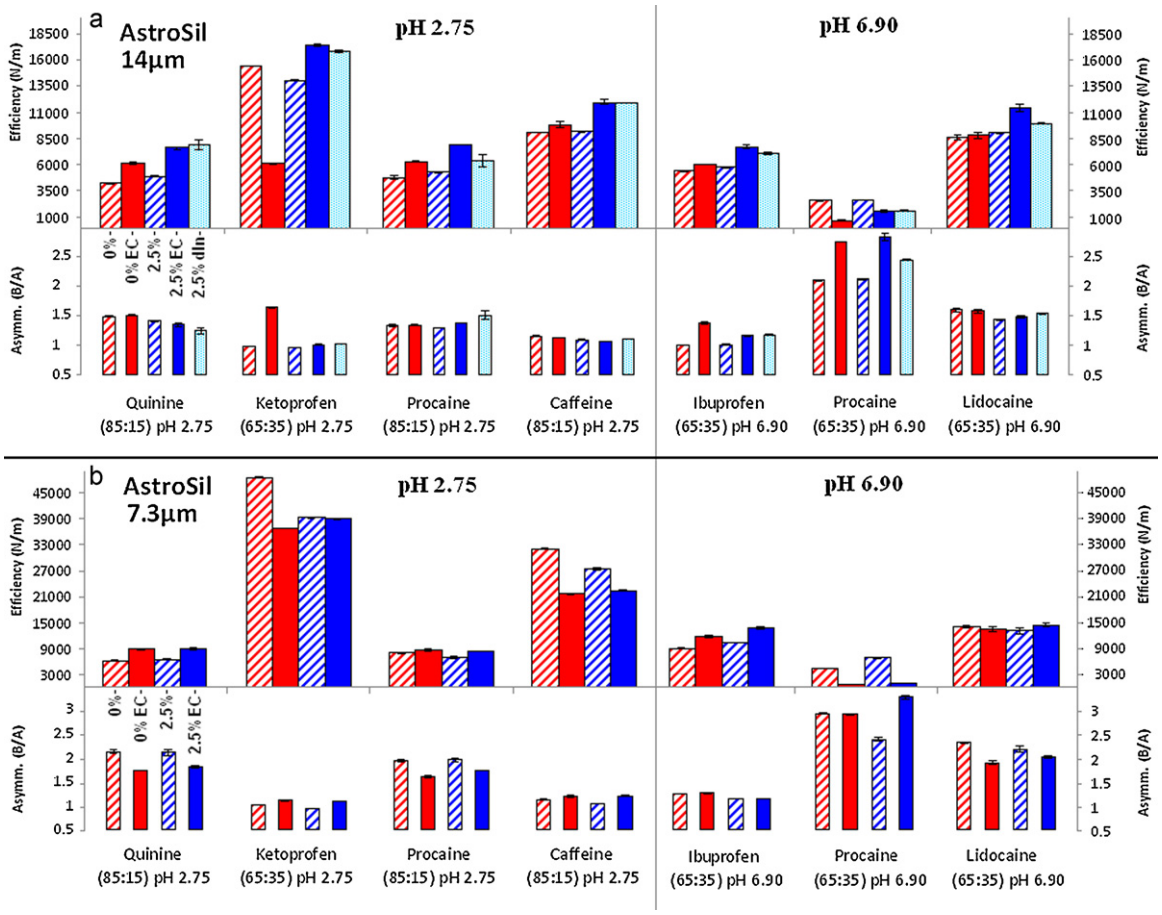

Fig. 5. Efficiency (upper plot, wide bars) and peak asymmetry at 10% peak height (lower plot, narrow bars) of eight drug analytes for (a) AstroSil 14 and (b) AstroSil 7.3 C18 phases. Stationary phases were both endcapped (solid) and non-endcapped (striped) at 0% pre-capping (red) and 2.5% pre-capping (blue). The 2.5% dilution phase "2.5%dln" is shown for AstroSil 14 (light blue). Same conditions as listed for Fig. 4. Error bars show the standard deviation of triplicate injections. (For interpretation of the references to color in this figure legend, the reader is referred to the web version of the article.)

ratio term, and the standard entropy of partitioning for a methylene group ($\Delta S^{\circ}_{-CH_2}$) can be calculated by Eq. (5).

$$\Delta S_{-CH_2}{}^{\circ} = \left[\left(\frac{\Delta S_e{}^{\circ}}{R} + \ln\varphi\right) - \left(\frac{\Delta S_t{}^{\circ}}{R} + \ln\varphi\right)\right] \times R \quad (5)$$

The results of the van't Hoff analysis are shown in Table 4. In general, the retention enthalpy for phenol, toluene, and ethylbenzene decreased in correlation with the carbon loading reported in Table 2. Most of the enthalpic changes for the two AstroSil phases were within the calculated error, but the Symmetry 5 material showed a more significant decrease. An interesting trend was observed in the entropy data, which consistently showed an increase in entropic favorability of retention with increased pre-capping. This effect was larger for the AstroSil 14 phase than the other two phases, with the 2.5%dln phase showing an identical entropy value as the 2.5% pre-capped phase. However, the calculated difference in retention entropies were minimal and within error of the van't Hoff linear regression.

Table 4
van't Hoff analysis results reported with standard error. Isocratic elution with 40:60 H_2O:ACN at 1.00 mL/min with uracil void marker. Temperature range from 15 °C to 55 °C (±0.05 °C) at 10 °C intervals, with triplicate injections at each temperature. All van't Hoff plots were linear with $R^2 \geq 0.99$. All phases were endcapped.

	% TMS pre-capping	ΔH° (kJ/mol)			$T\Delta S^{\circ}_{-CH_2}$ at 298 K (kJ/mol)
		Phenol	Toluene	Ethylbenzene	Ethylbenzene/toluene
AstroSil 14 µm	0%	−9.17 ± 0.10	−7.99 ± 0.18	−8.29 ± 0.23	0.67 ± 0.28
	2.5%	−9.28 ± 0.07	−7.92 ± 0.12	−8.17 ± 0.18	0.72 ± 0.21
	5.0%	−9.11 ± 0.10	−7.79 ± 0.11	−8.03 ± 0.16	0.72 ± 0.18
	7.5%	−9.19 ± 0.07	−7.89 ± 0.10	−8.11 ± 0.15	0.74 ± 0.18
	10.0%	−9.20 ± 0.08	−7.94 ± 0.11	−8.15 ± 0.17	0.76 ± 0.20
	2.5%dln	−9.15 ± 0.08	−7.87 ± 0.11	−8.10 ± 0.16	0.72 ± 0.19
AstroSil 7.3 µm	0%	−8.52 ± 0.05	−7.62 ± 0.16	−7.97 ± 0.21	0.65 ± 0.25
	2.5%	−8.38 ± 0.04	−7.48 ± 0.16	−7.80 ± 0.21	0.68 ± 0.25
Symmetry 5 µm	0%	−8.01 ± 0.14	−7.44 ± 0.11	−7.77 ± 0.16	0.65 ± 0.19
	2.5%	−7.48 ± 0.19	−7.05 ± 0.07	−7.35 ± 0.12	0.66 ± 0.13
	10.0%	−7.40 ± 0.17	−7.10 ± ± 0.06	−7.37 ± 0.11	0.67 ± 0.12

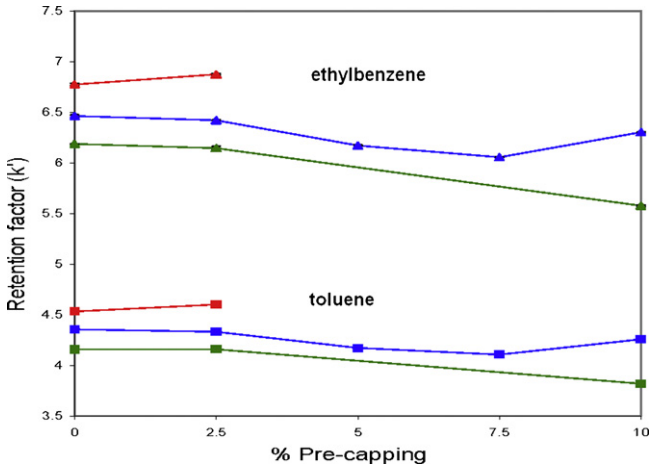

Fig. 6. Retention factor vs. pre-capping of ethylbenzene (▲) and toluene (■) for (a) AstroSil 7.3 (red), (b) AstroSil 14 (blue), and (c) Symmetry 5 (green). Isocratic elution with 40:60 H_2O:ACN at 1.00 mL/min at 25.0 ± 0.05 °C, 1:1 H_2O:ACN sample diluent, and uracil void marker. Error bars show the standard deviation of triplicate injections. All phases were endcapped. (For interpretation of the references to color in this figure legend, the reader is referred to the web version of the article.)

3.4. Stability

The limited temperature and pH range in which silica is chemically stable is often cited as a primary limitation of silica-based bonded phases. The rate of dissolution of the silica substrate under high pH and temperature conditions is directly related to the concentration of surface silanols accessible to hydrolysis by the solvent. In theory, if pre-capping yields a more evenly distributed bonded layer, this should shield the silica substrate more effectively than a heterogeneous bunching-type arrangement. The AstroSil 14 columns were subjected to forced degradation conditions with a 70% 0.20 M carbonate buffer (pH 10) and 30% methanol solution at 40 °C. At regular intervals, the columns were flushed-out with 50:50 H_2O:ACN, and aniline, toluene, and ethylbenzene were injected. The ethylbenzene results of this stability study are shown in Fig. 7. Retention decreased linearly ($R^2 > 0.996$), and the rate of retention loss was faster on phases with higher pre-capping. The efficiency for all phases was maintained until approximately 370–400 mL of degradation solution was flushed through, then it decreased drastically. Toluene and aniline exhibited identical trends in the loss of retention and efficiency upon degradation. These results indicate that pre-capping has a negative effect on the retention stability of silica bonded phases, most likely due to a decrease in carbon loading.

4. Conclusions

TMS pre-capping is still a viable method to improve analyte efficiency for Type-B monomeric C18 phases, however the effects on these phases are minimal. Analyte efficiency and peak shape improvements on Type-B phases were less in magnitude and occurred at a lower level of pre-capping as compared to those reported for Type-A silica. This supports the hypothesis that highly acidic silanols – their abundance, variation in reactivity, and their effects on bonded ligand heterogeneity – are primarily caused by metal contamination. In addition to impurity content, efficiency improvements may be dependant on the physical parameters of the silica substrate and how they affect bonded phase density.

Pre-capping at 2.5% gave a lower C-term for toluene compared to non-precapped phases, but improvements in efficiency were more significant for polar analytes under buffered conditions. However,

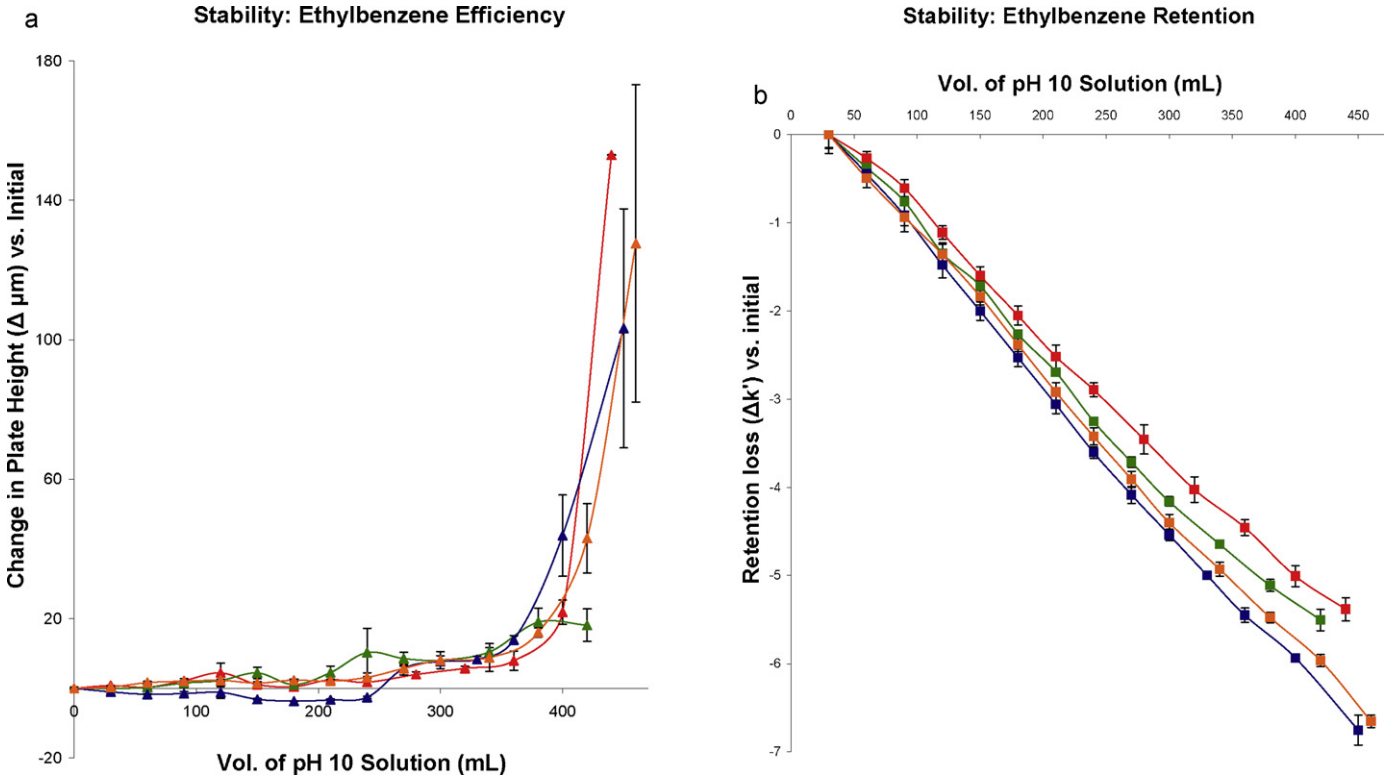

Fig. 7. AstroSil 14 pre-capping stability results showing (a) change in efficiency (▲), and (b) change in retention (■) of ethylbenzene vs. volume of degradation solution [0.20 M carbonate buffer pH 10: methanol (70:30)]. C18 phases at 0% (red), 2.5% (green), 5% (blue), and 7.5% (orange) pre-capping levels. Isocratic elution with 1:1 H_2O:ACN at 1.00 mL/min at 40.0 ± 0.05 °C, 1:1 H_2O:ACN sample diluent, and uracil void marker. Error bars show the standard deviation of triplicate injections. All phases were endcapped. (For interpretation of the references to color in this figure legend, the reader is referred to the web version of the article.)

due to the small difference in observed efficiencies in relation to the wide column-to-column variability, at present any improvements can only be described qualitatively. Also, pre-capped phases showed decreased carbon loading and less retention of non-polar analytes, as well as a slightly faster rate of retention loss under dissolution conditions. Therefore, it is concluded that pre-capping Type-B silica phases is best done at lower levels (∼2.5%) in order to maximize efficiency while minimizing loss of retention and stability. Future work will focus on silica phases of various pore sizes, alkyl ligand lengths, bonding densities, and lower pre-capping levels (<2.5%).

Acknowledgements

The authors wish to thank Dr. Albert Stiegman at Florida State University, Dr. Catherine Rimmer at NIST, Brad VanMiddlesworth at FSU, and Candace McGowan at the University of Pittsburgh for their insights and contributions to this project. Also, many thanks to Dr. Yingfeng Xu at the FSU/NHMFL Stable Isotope Lab in Tallahassee, FL for providing the %C elemental analysis data. This work was supported by the National Science Foundation, grant CHE-0717701.

References

[1] H.N.M. Stewart, S.G. Perry, J. Chromatogr. 37 (1968) 97.
[2] M.R. Buchmeiser, J. Chromatogr. A 918 (2001) 233.
[3] C.A. Doyle, J.G. Dorsey, in: E. Katz, R. Eksteen, P. Schoenmakers, N. Miller (Eds.), Handbook of HPLC: Chromatographic Science, Marcel Dekker Inc., New York, 1998, p. 293.
[4] L.C. Sander, S.A. Wise, CRC Crit. Rev. Anal. Chem. 18 (1987) 299.
[5] K.K. Unger, N. Becker, P. Roumeliotis, J. Chromatogr. 125 (1976) 115.
[6] A. Berthod, J. Chromatogr. 549 (1991) 1.
[7] U.D. Neue, in: R.A. Meyers (Ed.), Encyclopedia of Analytical Chemistry, Wiley, Chichester/New York, 2000, p. 11450.
[8] K.K. Unger, R. Skudas, M.M. Schulte, J. Chromatogr. A 1184 (2008) 393.
[9] K.K. Unger, Porous Silica: Its Properties and Use as Support in Column Liquid Chromatography, Elsevier, Amsterdam/New York, 1979.
[10] R.K. ller, The Chemistry of Silica: Solubility, Polymerization, Colloid and Surface Properties, and Biochemistry, John Wiley & Sons, New York/Toronto, 1979.
[11] G.B. Cox, J. Chromatogr. A 656 (1993) 353.
[12] D.V. McCalley, J. Chromatogr. A 1217 (2010) 858.
[13] J. Nawrocki, J. Chromatogr. A 779 (1997) 29.
[14] C. Stella, S. Rudaz, J.L. Veuthey, A. Tchapla, Chromatographia 53 (2001) S113.
[15] R.J.M. Vervoort, A.J.J. Debets, H.A. Claessens, C.A. Cramers, G.J. de Jong, J. Chromatogr. A 897 (2000) 1.
[16] H.A. Claessens, M.A. van Straten, J. Chromatogr. A 1060 (2004) 23.
[17] J.D. Sunseri, W.T. Cooper, J.G. Dorsey, J. Chromatogr. A 1011 (2003) 23.
[18] J. Nawrocki, Chromatographia 31 (1991) 177.
[19] J. Nawrocki, Chromatographia 31 (1991) 193.
[20] C.H. Lochmuller, A.S. Colborn, M.L. Hunnicutt, J.M. Harris, Anal. Chem. 55 (1983) 1344.
[21] D.B. Marshall, C.L. Cole, D.E. Connolly, J. Chromatogr. 361 (1986) 71.
[22] D.B. Marshall, K.A. Stutler, C.H. Lochmuller, J. Chromatogr. Sci. 22 (1984) 217.
[23] J.P. Foley, J.G. Dorsey, Anal. Chem. 55 (1983) 730.
[24] K. Miyabe, G. Guiochon, J. Chromatogr. A 830 (1999) 29.
[25] R.W. Stout, J.J. DeStefano, L.R. Snyder, J. Chromatogr. 261 (1983) 189.
[26] K.M. Usher, C.R. Simmons, J.G. Dorsey, J. Chromatogr. A 1200 (2008) 122.
[27] J.J. van Deemter, F.J. Zuiderweg, A. Klinkenberg, Chem. Eng. Sci. 5 (1956) 271.
[28] B. Buszewski, D. Berek, J. Garaj, I. Novak, Z. Suprynowicz, J. Chromatogr. 446 (1988) 191.
[29] B.W. Sands, Y.S. Kim, J.L. Bass, J. Chromatogr. 360 (1986) 353.
[30] T.L. Chester, J.W. Coym, J. Chromatogr. A 1003 (2003) 101.